Journal of Materials Chemistry A RSCPublishing

Supporting Information

Gradient dopant profiling and spectral utilization of monolithic thin-film silicon photoelectrochemical tandem devices for solar water splitting

Cite this: DOI: 10.1039/x0xx00000x

Received 00th September 2014,
Accepted 00th September 2014

DOI: 10.1039/x0xx00000x

www.rsc.org/

Lihao Han,[a,c]* Ibadillah A. Digdaya,[b] Thom W.F. Buijs,[a] Fatwa F. Abdi,[b]† Zhuangqun Huang,[c] Rui Liu,[c] Bernard Dam,[c] Miro Zeman,[a] Wilson A. Smith[b]* and Arno H.M. Smets[a]*

[a] Photovoltaic Materials and Devices (PVMD) Laboratory, Delft University of Technology, P.O. Box 5031, 2600 GA Delft, Netherlands.
* E-mail: L.Han@tudelft.nl, A.H.M.Smets@tudelft.nl
[b] Materials for Energy Conversion and Storage (MECS) Laboratory, Delft University of Technology, P.O. Box 5045, 2600 GA Delft, Netherlands.
* E-mail: W.Smith@tudelft.nl
[c] Joint Center for Artificial Photosynthesis (JCAP), California Institute of Technology, Pasadena, California, 91125, USA.
† Current address: Institute for Solar Fuels, Helmholtz-Zentrum Berlin für Materialien und Energie Gmbh, Hahn-Meitner-Platz 1, 14109 Berlin, Germany.

S1. Material optimization

The percentage of carbon atom number (C%) in the bulk material can be tuned through the methane/silane (CH_4/SiH_4) gas flow ratio. Under typical plasma enhanced chemical vapour deposition (PECVD) conditions SiH_4 molecules decompose much easier than CH_4 molecules. Therefore CH_4/SiH_4 gas flow ratios ranging from 1 to 20 are required to establish C% values in the a-SiC:H of ~10% up to 40%. In order to optimize the C% in our a-SiC:H material, we deposited 100 nm *i*-layers with different C% on Corning glass. The C% values were ~0%, ~10%, ~20%, ~30% and ~40% as confirmed by XPS (data not shown here), which was obtained by using CH_4/SiH_4 gas flow ratios of 0, 1, 3, 10 to 20, respectively.

In Table S1 the optical band gaps (determined from the measured reflectance and transmittance spectra) of the five a-$Si_{1-x}C_x$:H samples are presented. These results demonstrate that the higher the carbon content is, the larger the band gap is.

CH_4/SiH_4	Material	Bandgap (eV)
0	a-Si:H	1.79
1	a-$Si_{0.9}C_{0.1}$:H	1.81
3	a-$Si_{0.8}C_{0.2}$:H	2.11
10	a-$Si_{0.7}C_{0.3}$:H	2.28
20	a-$Si_{0.6}C_{0.4}$:H	2.47

Table S1 The CH_4/SiH_4 gas flow ratio injected in the plasma, the resulting percentage of carbon atom number (C%) and the optical bandgaps of the five a-$Si_{1-x}C_x$:H samples.

In order to study the presence of carbon and hydrogen in the material using Fourier transform infrared (FTIR) spectroscopy, we deposited the same five films (100 nm thick) on *p*-type crystalline silicon wafers. As shown in Figure S1, differences of C% in the bulk of the film can be revealed by the marked changes of the spectral signatures on the Fourier transform infrared (FTIR) spectra of this series of samples. The presence of carbon can be demonstrated by the absorption modes at 770 cm^{-1} corresponding to Si-C bonds and Si-CH_3 bonds and the modes at 1008 cm^{-1} corresponding to SiC-H_n bonds. These absorption peaks are indeed increasing with increasing values of C%. The surface silicon hydrides (Si_y-H_x) bonds have various stretching modes: Si-H bond low stretching mode (LSM)[1] at 2000 cm^{-1} corresponding to hydrides in small volume deficiencies (vacancies) Si-H bonds Si-H high stretching mode (HSM)[2, 3] at 2070-2100 cm^{-1} corresponding to hydrides at the surface of nano-sized voids. For increasing C% the HSM increases and the LSM decreases. This shows that the incorporation of carbon results in more porous materials due to the incorporation of more nano-sized voids. Higher densities of nano-sized voids create more defects in the films and reduce the PEC performance of this material.

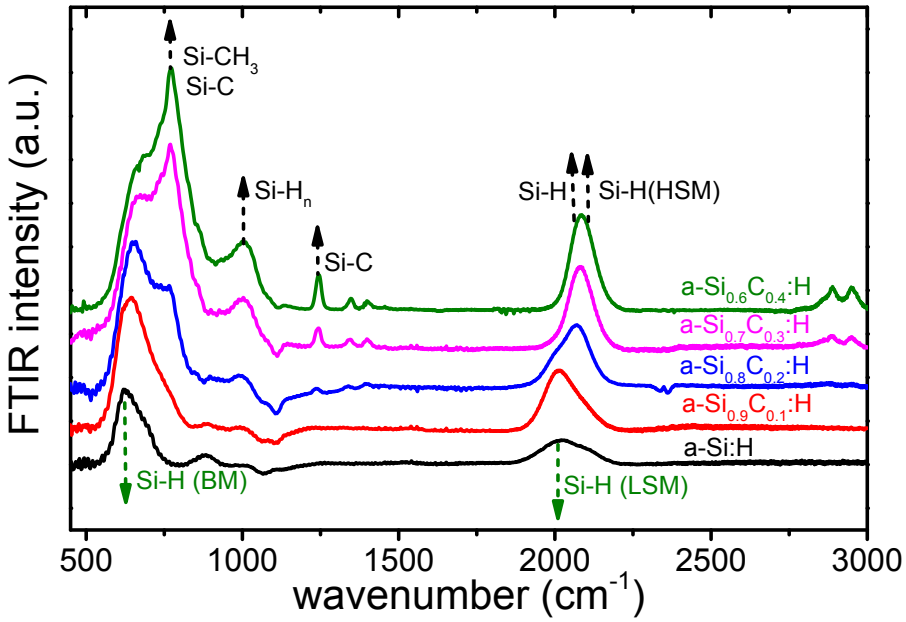

Fig. S1 Fourier transform infrared (FTIR) spectra of i-a-SiC:H films with different C% and bandgap.

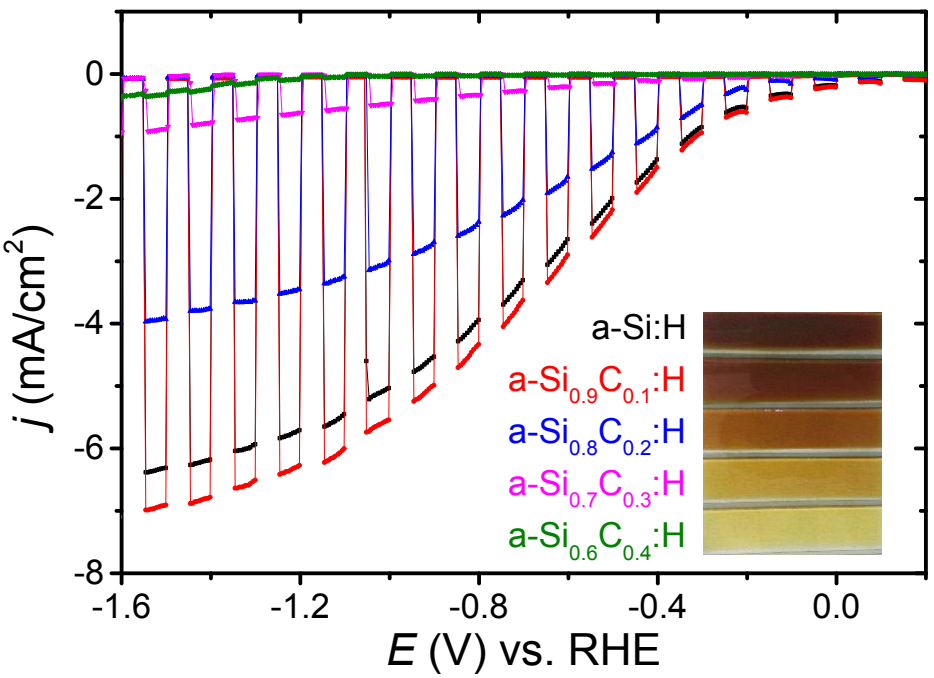

Fig. S2 PEC measurements of the photocathodes in the series of C% in the *i*-a-SiC:H layer. The inset photo shows less sunlight is absorbed in the C-rich samples.

Five photocathodes consisting of 10 nm *p*-a-SiC:H layer and 100 nm *i*-a-SiC:H layer were prepared, where C% of *i*-a-SiC:H layer was varied ~0, ~10, ~20, ~30, and ~40%. The inset photo in Figure S2 shows how the colours of these electrodes change from dark brown to yellow as C% increases. This is consistent with the subsequent bandgap widening as shown in Table S1. Figure S2 also demonstrates the increase of C% deleteriously affects the current densities of these electrodes. For example, the photocurrent density at -1.5 V *vs.* RHE changed from -7.0 mA cm^{-2} (10% C) to -0.35 mA cm^{-2} (40% C). This is a result of both the band gap widening which results in reduced photon absorption and an increased density of defects which serve as charge recombination centres. Due to its ideal band gap and stability the *i*-a-SiC:H layer with 10% carbon incorporated was selected in the fabrication of the PEC/PV configuration.

S2. Glass substrate with integrated micro-textured photonic structures

Using textured substrates is the conventional approach to enhance the light trapping in PV devices.[4, 5] However, a delicate interplay exists between textured substrates and the growth of device grade PV materials on top. Especially, nc-Si:H is highly sensitive to extreme texture, as the texture initiates the growth of defect rich filaments above sharp valleys during growth.[6] The size and density of these defect-rich filaments grow with thickness. These filaments significantly reduced the fill factor (*FF*), open circuit voltage and current density of the PV junctions.[6, 7] However, the PEC/PV device needs thick (> 3 µm) nc-Si:H bottom cells to achieve the required high spectral utilization. To prevent the incorporation of defect-rich filaments and to allow the integration of thick high quality nc-Si:H junctions in our PEC/PV devices, state-of-the-art glass substrates with integrated micro-textured photonic structures have been used. These photonic structures have been obtained by wet-etching a sacrificial ITO layer on Corning glass, resulting in craters with typical diameters in the order of 10 µm and depths of 2 µm. A back reflector consisting of aluminum doped zinc-oxide (AZO, 2 µm) / metal reflector (30 nm Cr + 100 nm Ag)/ AZO (10 nm) has been deposited on top. Besides the micro-texture, the back reflector has nano-textured photonic structures as well (Figure S3), as a result of the natural growth of the AZO. The PEC and PV junctions deposited on top adopt the nano-textured and micro-textured photonic structures. The nano-scale photonic structures facilitate the light scattering of the high energetic photons in to the a-SiC:H photocathode, while the micro-scale photonic features facilitate an efficient light trapping in the TF-Si PV junctions in the red and near infrared spectral range.[7] As demonstrated in the SEM image in Figure 1 (b), the glass substrate with micro-textured photonic structures allows the growth of highly dense nc-Si:H material. No defect-rich filaments can be observed in the 4 µm thick nc-Si:H material, which guarantees high voltages and current densities in the PV junction of the PEC/PV device.

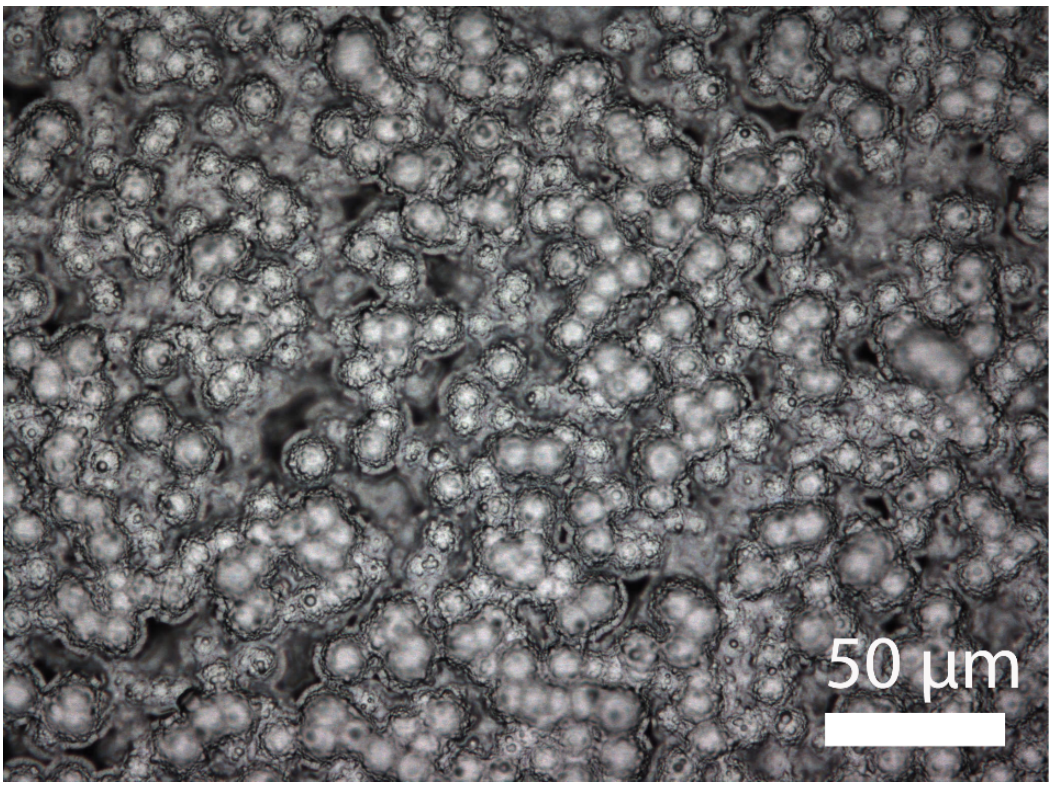

Figure S3 Microscopy image of the nano-textured AZO on the surface of the micro-texture glass as the substrate for the PEC/PV cathode.

S3. Electrochemical impedance spectroscopy (EIS)

The flat band potential and the acceptor density of the a-SiC:H photocathode with an active area of 0.283 cm^2 were characterized by electrochemical impedance spectroscopy (EIS). In order to obtain an accurate Mott-Schottky analysis, the scanning frequencies should be chosen in the range that the real part of the impedance is constant and only the imaginary part of the impedance is varied ($\log(-Z_{im})$ *vs*. $\log(f)$ has a slope of -1). Thereby, the imaginary impedance can be fully interpreted as the contribution from the space charge layer capacitance. Based on the Bode and Nyquist plot, the frequency range for our a-SiC:H photocathode is 500 Hz. The following Mott-Schottky equation then applies:

$$\frac{1}{C_{sc}^{\ 2}} = -\frac{2}{\varepsilon_0 \varepsilon_r e N_A A^2}\left(V - V_{\mathrm{fb}} - \frac{k\mathrm{T}}{e}\right) \quad (1)$$

Based on Equation (1), the x-axis and the slope of the Mott-Schottky plot can be used to determine the flat band potential (V_{fb}) and the acceptor concentration (N_{A}), respectively. Figure S4 shows the Mott-Schottky plot for our a-SiC:H photocathode at 500 Hz under dark condition.

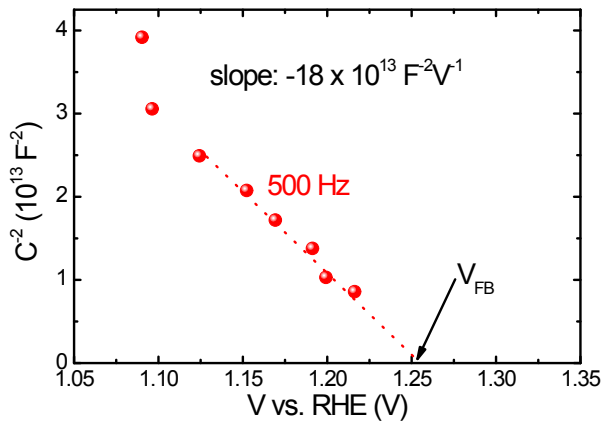

Figure S4 Mott-Schottky plot of the a-SiC:H film at 500 Hz, taken under dark condition

The V_{fb} is estimated to be ~1.25 V vs. RHE, and the N_A is approximated to be 2.5 × 10^{17} cm^{-3}, assuming a dielectric constant of 14. The valence band edge E_V could be determined using the following relationship:

$$E_F - E_V = -kT \ln\left(\frac{N_A}{N_V}\right) \quad (2)$$

where the effective density of valence band states

$$N_V = 2\left(\frac{2\pi m_h^* kT}{h^2}\right)^{3/2} \quad (3)$$

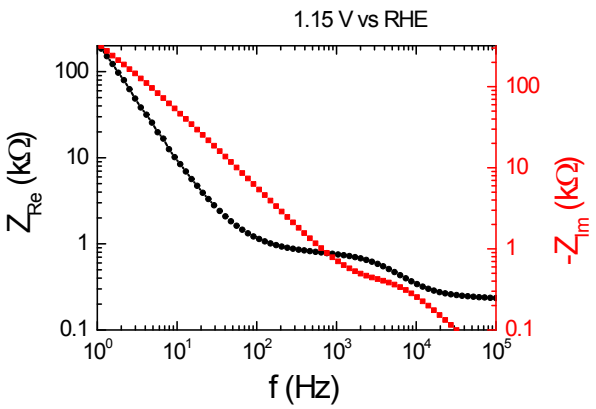

(a)

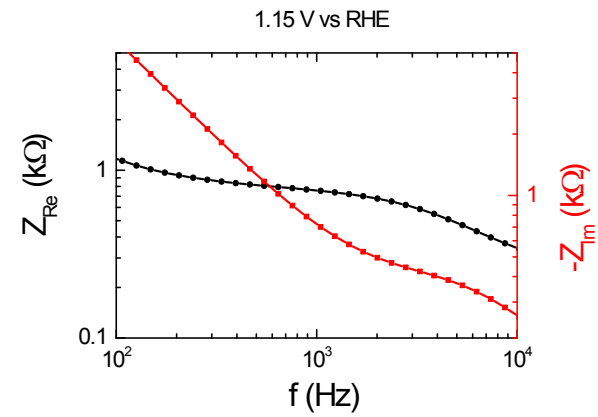

(b)

Figure S5 Real and imaginary impedance as a function of frequency in the frequency range of 1-10^5 Hz (a) and the magnification part in the frequency range of 10^2-10^4 Hz (b).

The effective mass of hole (m_h^*) of $0.3m_0$ is assumed to be similar to that c-Si and the effective density of valence band states (N_V) is calculated to be 4 × 10^{18} cm^{-3}. This calculation suggests that the Fermi level is located 80 mV above the valence band edge.

1 A. H. M. Smets, W. M. M. Kessels and M. C. M. van de Sanden, *Appl Phys Lett*, 2003, **82**, 1547-1549.
2 G. Lucovsky, R. J. Nemanich and J. C. Knights, *Phys Rev B*, 1979, **19**, 2064-2073.
3 D. V. Tsu, G. Lucovsky and M. J. Mantini, *Phys Rev B*, 1986, **33**, 7069-7076.
4 C. Battaglia, C. M. Hsu, K. Soderstrom, J. Escarre, F. J. Haug, M. Charriere, M. Boccard, M. Despeisse, D. T. L. Alexander, M. Cantoni, Y. Cui and C. Ballif, *Acs Nano*, 2012, **6**, 2790-2797.
5 K. Jager, O. Isabella, L. Zhao and M. Zeman, *Phys Status Solidi C*, 2010, **7**, 945-948.
6 M. Python, E. Vallat-Sauvain, J. Bailat, D. Domine, L. Fesquet, A. Shah and C. Ballif, *J Non-Cryst Solids*, 2008, **354**, 2258-2262.
7 H. Tan, L. Sivec, B. J. Yan, R. Santbergen, M. Zeman and A. H. M. Smets, *Appl Phys Lett*, 2013, **102**, 153902.